60-Gb/s Mode Division Multiplexing and Wavelength Division Multiplexing in Si Multimode Waveguides

Christine P. Chen(1)*‡, Jeffrey B. Driscoll(1)*, Richard R. Grote(1), Yue Liu(1), Richard M. Osgood, Jr.(1), Keren Bergman(1)

(1)*Dept. of Electrical Engineering, Columbia University, New York, NY*
**These authors contributed equally to this work.*
‡*christinechen@ee.columbia.edu*

Abstract. A silicon photonic waveguide system with mode-division and wavelength-division-multiplexing capabilities is demonstrated. Error-free (BER $< 10^{-12}$) data transmission of 2 modal channels and 3-wavelengths operating with aggregate bandwidth of 60-Gb/s is realized. This work motivates future bandwidth scalability of silicon photonic interconnects.

1. Introduction

As high-performance computing systems continue to increase in functionality and speed, sustained growth in data rate is beginning to reach a saturation point due to the bandwidth bottleneck of current microelectronic systems. Silicon photonics make possible a multifold increase of bandwidth, while technological advances have yielded low-loss waveguide structures.

The motivation for transitioning from electronic to optical interconnects is driven by the need to increase bandwidth while keeping power cost minimal. Utilizing the high bandwidth of silicon photonics will make possible the continuation of this computing trend. Paramount for transitioning in this direction is the smooth integration of photonic devices into existing systems, as illustrated conceptually in (Fig. 1). Low insertion loss is maintained through engineering the geometry of the device and its effective index [1]. Previous experiments have demonstrated terabit-speed communication capabilities [2] using wavelength-division multiplexing (WDM). These feature CMOS-compatible photonic devices that enable high-bit rates for high-performance computing centers [3].

A promising way to increase data rates without sacrificing small area is via multi-mode devices (MMD). These add an orthogonal dimension to the operational regime, thereby increasing data rates considerably for a given spatial density. Transmission of multiple channels in these systems occurs along a single path by combining signals on independent modes using a mode-multiplexer, which is then received separately at the output using a mode-demultiplexer.

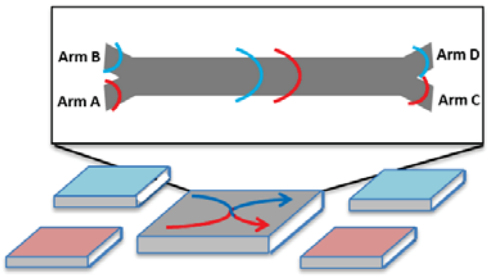

Figure 1. Data transmitted on Quasi-TM mode traverses from A to C and B to D, conceptually integrated into a multi-node system.

In this work, a full system demonstration of a silicon photonic interconnect with 2 modal channels and 3 wavelengths operating simultaneously is shown. Operation occurs with an aggregate bandwidth of 60 Gb/s, with $<$ 1 dBm power penalty in this system.

2. Silicon Waveguide

An asymmetric Y-junction device, described in greater detail in [4], was used in this experiment as a mode multiplexer and demultiplexer. The dimensions of the height and width of each arm are 250 nm by 450 nm for arm A, 250 nm by 550 nm for arm B, and 250 nm by 1 um for the multimode interconnect links, with a branch angle of 3 degrees. For this chosen angle and for quasi-transverse-magnetic (QTM) excitation, the device is outside the mode-sorting regime [4,5]; thus, each input channel is spread over both modes of the multimode waveguide by the multiplexer. However, from the property of time reversal symmetry

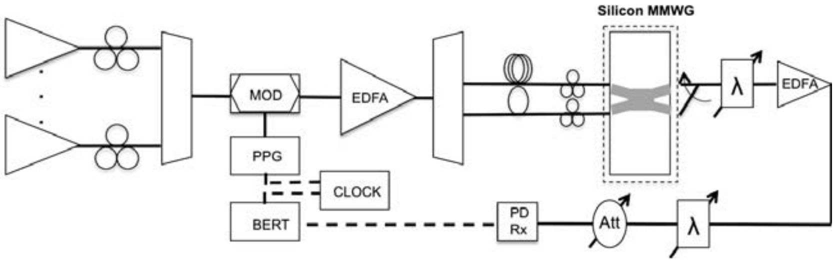

Figure 2. Experimental setup

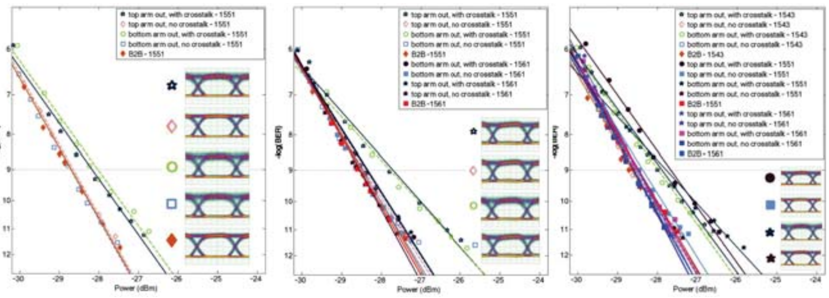

Figure 3. BER Measurement with 1 (left), 2 (middle), and 3 (right) operating wavelengths. Eye diagrams correspond to items at 1555 nm.

it is known that each individual channel can still be demultiplexed with low crosstalk at wavelengths where the relative phase difference ($\Delta\phi_{e,o} = \phi_e - \phi_o$) between the even ($\phi_e$) and odd ($\phi_o$) modes of the waveguide equals an integer multiple of 2π [4]. Using this approach, more compact devices can achieve even lower crosstalk! in the demultiplexer.

3. Experimental Setup and Results

The experimental setup (Fig. 2) for the BER measurements of 1, 2, and 3 operating wavelengths, with and without both arms operating simultaneously (with and without crosstalk), along with the respective eye diagrams for 1551 nm operation (Fig. 3) begins with the combination of two continuous-wave (CW) tunable lasers operating at 1551 nm and 1561 nm and one distributed feedback laser operating at 1541 nm, using a 3-to-1 multiplexer. This signal is then modulated with a modulator and pulse-pattern generator (PPG) to generate a non-return-to-zero (NRZ) 2^7-1 pseudo-random bit sequence (PRBS) signal. Then, it is amplified by an erbium-doped fiber amplifier (EDFA) before being passed through a 1.5 km spool of standard single-mode fiber (SSMF) to decorrelate the wavelength channels by $\sim$ 25 ps/nm. An inline power splitter splits the signals into two channels, and a decorrelating SSMF of 100 m was used to provide a many-bit delay between the two signals. Each path has a pol! arization controller (PC), polarizer, and another PC to control the polarization of each arm separately to ensure QTM mode excitation in the waveguide. A pitch reducing optical fiber array (PROFA) with 38 um pitch was used to simultaneously inject both input Y-junction arms with a separate data channel at each wavelength. The EDFAs are adjusted to ensure a launch power of $\sim$ 10 dBm. The signal exiting the chip is alternately taken from the upper or the lower arm using a lensed tapered fiber, with around 28 dBm insertion loss, which was the same for both arms. This signal is filtered using a tunable filter to isolate a single wavelength channel and suppress amplified spontaneous emission (ASE) from the EDFA on the input side. Then, it is amplified by a low-noise-figure EDFA and filtered again to reduce ASE noise. The signal is passed into a variable optical attenuator (VOA) to attenuate it over a range of powers for bit error rate (BER) measurements. The optical signal w! as received and converted to an electrical signal using a PIN-! TIA avalanche photodetector (PD) followed by a limiting amplifier (LA) to amplify the signal going into the BER tester. A digital communications analyzer (DCA) was used to record eye diagrams, and the chip was bypassed for back-to-back comparison.

When transmitting several wavelengths along the two modal channels (MDM-WDM) the amount of crosstalk leaking from one modal channel to the

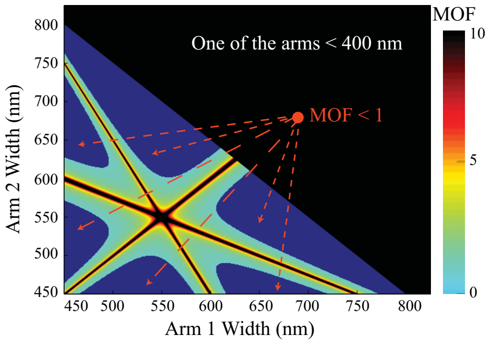

Figure 4. Asymmetric Y-junction design space according to (1) assuming $\theta = 0.5$ degrees, a multimode interconnect width (w_{mm}) of $w_{mm} = 1.65\ \mu$m , and the width of arm 3 (w_{a3}) is $w_{a3} = w_{mm} - w_{a1} - w_{a2}$. Blacked-out regions indicate a geometry that results in one arm width being < 400 nm. Dark blue regions represent designs where MOF < 1, representing effective 3×3 mode multiplexer designs.

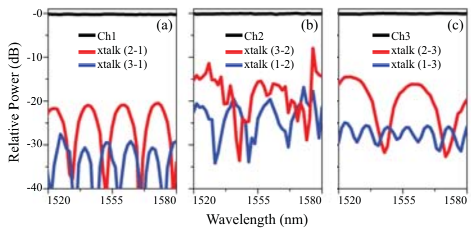

Figure 5. Image illustrates a theoretical spectral scan of a 3-mode device with 0.5 degree Y-junction angles simulated using the design methodology described in [5] with geometry 250 nm $\times$ 450 nm for arm 1, 250 nm $\times$ 520 nm for arm 2 and 250 $\times$ 680 nm for arm 3. The interconnect cross section is 250 nm $\times$ 1.6 μm and is 1 mm long.

next at each wavelength was minimized by choosing the spectral regions that exhibited minimal crosstalk [4]. Then, by balancing the power entering each arm at a particular wavelength such that the relative crosstalk of each channel is equal, minimally equivalent crosstalk performance could be realized.

By looking at Fig. 3, the level of crosstalk per channel can be seen. The experimental results of a single-wavelength MDM, dual-wavelength MDM-WDM, and triple-wavelength MDM-WDM are displayed. From these curves, the power penalties for 1551 nm at BER = 10^{-9}, when averaged between top and bottom arms, turn out to be 0.6 dB for 1 wavelength, 0.66 dB for 2 wavelengths, and 0.7 dB for 3 wavelengths.

4. Extending Modes for Mux-Demux Operation

While data communication in a two-mode interconnect has been demonstrated here, it is possible to scale the mux-demux operation to a higher number of modes. The optimal regime for a 3×3 asymmetric Y-junction can be found using the design methodology of [5], which approximates the device geometry that minimizes a multiple output factor (MOF), defined as

$$\text{MOF} = \theta \sum_{i=1}^{N} \sum_{j>i}^{N} \left| \frac{i-j}{\beta_i - \beta_j} \right| \gamma_{ij} \tag{1}$$

where N is the number of arms, i and j denote individual arms, θ is the divergence angle between adjacent arms (in radians), $\beta_{i,j}$ is the propagation constant of the fundamental mode of an arm, and γ_{ij} is the evanescent decay constant of the fundamental mode between two arms. To verify this design, the crosstalk in each arm is modeled as a function of wavelength using both the effective index method and 2-d eigenmode expansion method and found to be < 10 dB across the C-band, with a minimal value of -25 dB for each arm. With this design, 3-mode MDM could be performed at multiple wavelengths with power penalties < 1 dB.

5. Conclusion

An experiment operating a MDM-WDM system with error free performance is demonstrated. In the shift towards integrating silicon photonics into current communications and computing systems, devices like this illustrate functional high bit rate capability through the use of a spatially small 2x2 MMD device. The described system motivates all-Si, low-loss on-chip optical interconnects. Further work could focus on improving device characteristic for supporting more modes in an effort to reach higher data rates.

Acknowledgements

This work was supported in part by the Interconnect Focus Center, a Semiconductor Research Corporation (SRC) and DARPA program, as well as from NSF and Semiconductor Research Corporation under Grant ECCS-0903406 SRC Task 2001 and the Semiconductor Research Corporation Master's Scholarship. Research was carried out in part at the Center for Functional Nanomaterials, Brookhaven National Laboratory, which is supported by the U.S. Department of Energy, Office of Basic Energy Sciences, under Contract No. DE-AC02-98CH10886.

References

[1] T. Uematsu *et al.*, *Journal of Lightwave Technology*, **30**, 15 (2012).
[2] B. Lee *et al.*, *Photonics Technology Letter, IEEE*, **20**, 6 (2008).
[3] A. Shacham *et al.*, *IEEE Transactions on Computers* **57**, 9 (2008).
[4] J. Driscoll *et al.*, *Optics Letters* (2013) (to be published).
[5] N. Riesen *et al.*, *Appl. Opt. 51* **51**, 15 (2012).